Development of a modular concrete heliostat prototype

Cite as: AIP Conference Proceedings **2445**, 120013 (2022); https://doi.org/10.1063/5.0086016
Published Online: 12 May 2022

Patrick Forman, Sebastian Penkert, Andreas Pfahl, et al.

Development of a Modular Concrete Heliostat Prototype

Patrick Forman[1, a)], Sebastian Penkert[2], Andreas Pfahl[3], Jürgen Schnell[2] and Peter Mark[1]

[1]*Ruhr University Bochum, Institute of Concrete Structures, Universitätsstraße 150, 44801 Bochum, Germany*
[2]*Technical University of Kaiserslautern, Institute of Concrete Structures and Structural Engineering, Paul-Ehrlich-Straße, Building 14, 67663 Kaiserslautern, Germany*
[3]*German Aerospace Center (DLR), Institute of Solar Research, Solar Power Plant Technology, Professor-Rehm-Str. 1, 52428 Jülich, Germany*

[a)]Corresponding author: patrick.forman@rub.de

Abstract. The main idea of this contribution is to replace typical steel structures for heliostats by means of concrete due to its low costs. With respect to accuracy demands, a high-performance concrete is used that possesses high compressive and tensile strengths. The collector is designed as a strut-like structure with main radial beams and a central mount to ensure high stiffness. The design exhibits a circular shape to reduce shading. For construction, the concrete collector is dissolved into equal modules derived from symmetry reduction methods enabling a serial production. To show the feasibility, a small-scale prototype with a diameter of 3.2 m and a mirror area of 8 m² is developed that will be built up and qualified at the solar power tower Jülich, Germany. It consists of 4 modules and exhibits a weight of 341 kg.

INTRODUCTION

Concentrated solar power (CSP) possesses an installed power of about 6 GW worldwide [1]. Next to parabolic trough collectors, which are the most established CSP systems, the most promising technologies are point-focusing solar power tower plants that use heliostats to focus the direct solar radiation onto a receiver. To be competitive on market, the developments of heliostat collectors are yielding for cost effectiveness, since their investment costs exhibit up to 40 % of the total CSP plant [2]. Apart from the drives, the supporting structure thereby offers the highest potential for cost reductions. For a holistic evaluation of the heliostat costs, also the construction as well as installation with respect to the environmental conditions have to be considered. However, the investigations presented here focus onto the development of an lightweight concrete concentrator prototype.

Up to now, heliostats are typically built up as T-type steel structures. Thereby, mirror elements are supported by cross beams. These beams are mounted to a torque tube enabling the tilting of the concentrator. A pylon supports the torque tube. Main disadvantage of this type is the superimposition of deformations from the cross beams and the torque tube. However, one of the most advanced heliostats is the Stellio developed by schlaich bergermann partner (sbp) [3], which exhibits a central mount and radial cantilever arms. Doing so, the load path is reduced in comparison to T-type heliostats and the steel framework cantilever arms are evenly utilized. Due to its high optical accuracy, it serves as a benchmark for the concrete design.

In this contribution, the main idea is to replace steel structures for heliostats by means of concrete due to its low costs. For parabolic troughs, shell-like concrete structures made from high-performance concrete (HPC) have already proven to be an alternative to conventional collectors [4,5]. These shells will now be dissolved in strut-like structures for heliostats. Doing so, the statical height is increased ensuring higher stiffness with respect to higher accuracy demands that come along with heliostat structures. The conceptual design of the concrete collector is orientated at the Stellio [3]. Main bearing elements are radial beams and a central mount is chosen. An inner ring connects the radial beams and transfers the loads to the support. For a compact field layout [6], the heliostat exhibits

SolarPACES 2020
AIP Conf. Proc. 2445, 120013-1–120013-8; https://doi.org/10.1063/5.0086016
Published by AIP Publishing. 978-0-7354-4195-8/$30.00

a circular shape with an outer ring. Secondary strut elements serve as an additional support of the mirror elements. The design is derived as a modular structure (cf. Figure 1).

To demonstrate the feasibility, a prototype has been developed as a small-scale collector. Its outer dimensions are adjusted to the heliostat types of the pilot solar power plant in Jülich (Germany), where it will be built up and qualified. The heliostat exhibits a diameter of 3.2 m resulting into a mirroring aperture of 8 m² (Figure 1). The focal length is set to 92 m which results into a height of the paraboloid surface of 7 mm.

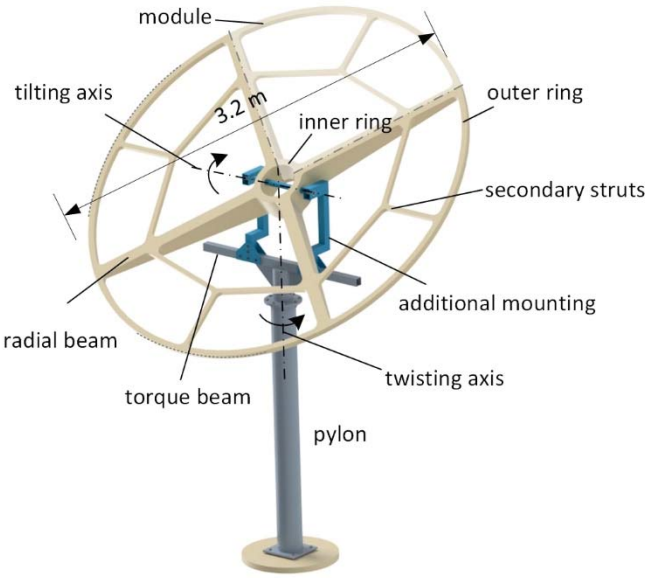

FIGURE 1. Digital twin of the concrete heliostat

CONCEPTUAL DESIGN

High-Performance Concrete

The used HPC is based on the binder Nanodur® Compound 5941. This type of concrete is typically used for machine beds due to its high precision demands. It exhibits a self-compacting behavior, high durability and good workability [7]. Hence, it is particularly suitable for the environmental conditions of typical solar power plant locations. Among a high compressive strength of >100 MPa, the HPC possesses a pronounced flexural tensile strength of 20 MPa in average. The high tensile strength is crucial to ensure a non-cracked structure, since softening by cracking would cause enlarged deformations. Moreover, the Young's modulus of about 50,000 MPa is much higher than the one of regular concrete which also is advantageous for low deformations. The concrete parameters used for the design are summarized in Table 1. In comparison, regular concrete exhibits a maximum Young's modulus E_{cm} of 37,000 MPa, a mean (cylinder) compressive strength f_{cm} of up to 58 N/mm² and a tensile strength f_{ct} of <3 N/mm².

TABLE 1. Material properties of Nanodur® concrete for the design (Subscripts: c – concrete, m – mean, t – tension, fl – flexural)

Description	Value	Unit
Young's modulus E_{cm}	50,000	MPa
Compressive strength f_{cm}	116	N/mm²
Flexural tensile strength $f_{ctm,fl}$	20	N/mm²
Reduced axial tensile strength f_{ct}	6.6	N/mm²
Bulk density γ_c	25	kN/m³

Action Effects

The specific action effects vary with the position of the collector. They mainly consist of deflection-related dead and wind loads.

Dead Loads

The dead loads mainly arise from the concrete structure with a bulk density of 25 kN/m³ (cf. Table 1). Additionally, the mirror elements have to be accounted for. For mirroring, the composite elements 'vegaprime' by Almeco are used that consist of a top and a bottom aluminum layer with a plastic core. With respect to accuracy demands, a composite thickness of 2 mm is chosen. It exhibits a weight of 2.9 kg/m².

Wind Loads

The wind loads are gained from wind tunnel test [8-10] for rectangular collectors. For the design of the concrete concentrator, pressure distributions coefficients with respect to the collector position acc. to [9] are adapted and simplified for the circular shape. To account for inaccuracies of this simplified model a safety factor of 2 is applied. Moreover, the resulting force and moment coefficient are evaluated to determine the load impacts on the substructure. They show good accordance with the results in [10]. However, for a more detailed wind load distribution onto the circular heliostat, wind tunnel tests or CFD analysis are suggested. For a first demonstrator, the simplified but by means of an increased partial safety factors adjusted wind load approach seems to be sufficient.

Moreover, a differentiation between operation and survival state is made. In operation state, the collector orientation is variable with moderate wind speeds of up to 10 m/s, whereby in survival state the heliostat is fixed in stow position (horizontal mirror panel) with wind speeds of 33 m/s.

Accuracy Demands

The optical efficiency crucially depends on an undisturbed mirror surface. Due to the loads, deformations of the concrete structure and mirror surface occur that cause slope deviations *SD*. For a qualification of the accuracy, the root mean square (rms) value of *SD* is widely used. For the design, the limit value is orientated on the Stellio heliostat with a SD_{rms} of 1.25 mrad [3]. This value holds true for the assembled collector. Here, a separation between *SD* from bending, i.e. deformations of the concrete structure, and from waviness, i.e. deformations from the mirror elements, is made. The accuracy criterion is therefore defined by the square root of the squared sum of both shares:

$$SD_{rms} = \sqrt{SD_{rms,bending}^2 + SD_{rms,waviness}^2} \leq 1.25 \quad (1)$$

With an equal weighted approach, the limiting value for the concrete structure, as well as for the mirror surface, corresponds to $SD_{rms,bending}$ = 0.88 mrad.

Symmetry Reduction Method

Heliostats made from concrete are mainly loaded due to its self-weight. This means, they are mainly stressed in horizontal position and the survival state appears as the dominant load situation. Additionally, heliostats exhibit a low curvature based on their high focal length. Hence, the concrete heliostat can be idealized as rotationally symmetric plate with a pointwise central mount. By means of symmetry reduction methods [11,12], this plate can then be represented by a cantilever arm with a length of the radius *R* (Figure 2 For the form-finding of the heliostat, the plate can be divided into segments defined by the angle φ and transferred into stiffness-equivalent radial beam elements. These segments define the modules to be built.

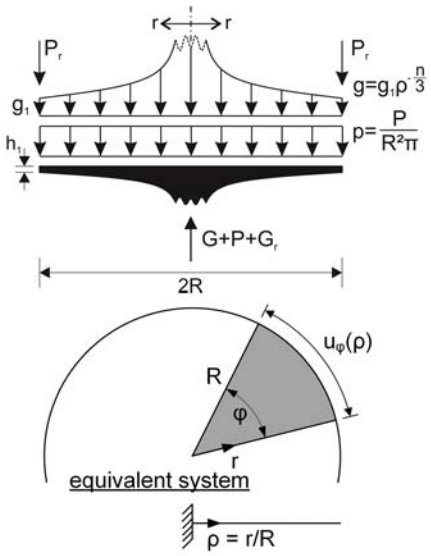

FIGURE 2. Rotationally symmetric plate with hyperbolical thickness and loads with equivalent partial structure and statical system of a plate

The height of the plate has a hyperbolical increasing curvature defined by the height h_1 at the edge and the shape factor n. With the dimensionless coordinate ρ, defined as the ratio between the radial coordinate r and the radius R, the plate thickness is described by [11]:

$$h(\rho) = h_1 \rho^{-n/3} \tag{2}$$

The shape factor is chosen to $n = 2$ that results in a reduced plate thickness and consequently weight.

For the aimed segmentation of the plate, the equivalent (radial) moment of inertia $\tilde{I}_r$ can be derived with respect to the angle φ:

$$\tilde{I}_r = \frac{1}{12} R h_1^3 \rho^{1-n} \varphi \tag{3}$$

In a next step, loads are applied on the plate as shown in Figure 2 (top). Hereby, g corresponds to the self-weight of the plate, p is an area load and P_r a line-like load representing the outer ring. The self-weights g and P_r are defined by the concrete's bulk density (cf. Table 1) and the area load p is simplified to 0.5 kN/m² representing the wind loads and mirror elements.

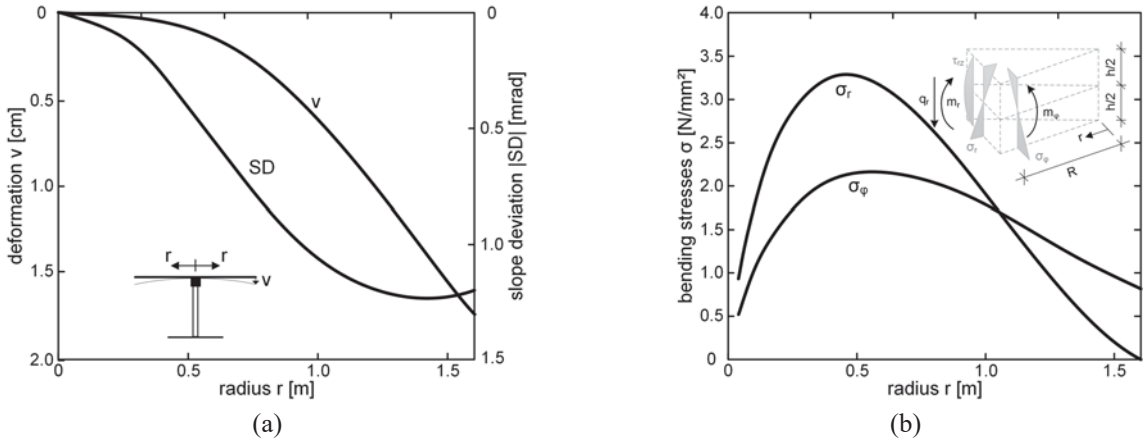

FIGURE 3. (a) Deformation v and slope deviation SD of the plate; (b) Bending stresses σ

Steered by the height h_1, deformations v and bending moments m of the plate can be determined. The deformations are transferred into slope deviations SD – being the gradient of deformations – (Figure 3a) and the bending moments into stresses (Figure 3b). By means of spreadsheet analyses, the height h_1 is adjusted so that the restrictive slope deviation value of $SD_{rms} \leq 0.88$ mrad, which results from the course of SD in Figure 3a, and the restrictive axial stress of $\sigma \leq 6.6$ MPa are complied with. Hereby, the limiting slope deviation SD_{rms} turns out to be the dominant restriction.

Since the height of the plate is obtained, the plate is divided into 4 modules defined by an angle of $\varphi = 90°$. Thereby, the stiffness of the plate is determined according to Eq. 4 with respect to the partial elements size. Now, stiffness-equivalent radial beams are derived, whereby a beam width of $w = 10$ cm is chosen. The height of the plate and beam as well as the equivalent moment of inertia are shown in Figure 4. The greyed-out area represents the inner ring where the radial beams meet and are rigidly connected to an inner steel ring.

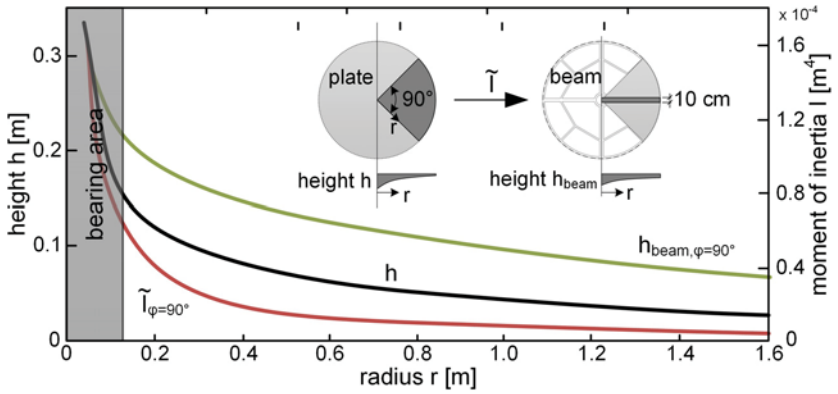

FIGURE 4. Transformation of the plate thickness to a beam with equivalent stiffness: Height of the plate (black line), equivalent moment of inertia (red line) and resulting beam height (green line)

Structural Design

For the structural design, the radial beams are linearized with respect to manufacturing demands. Additionally, the inner and outer rings as well as secondary struts – for stability constraints and mirror support – enhance the strut-like model (cf. Figure 1). The geometric parameters of the struts are summarized in Table 2. The weight of the concrete structure exhibits 341 kg which corresponds to 85 kg per module.

TABLE 2. Geometric parameters of the struts

Description	Width [cm]	Height [cm]
Radial beams	10	23-5
Inner ring	5	23
Outer ring	5	5
Secondary struts	4	4

The heliostat is built up as a numerical model in the Finite Element software ANSYS consisting of the concrete structure and mirror elements. For accuracy analysis, the deformations are derived with the maximum wind loading in operation state. However, a horizontal position of the mirror panel is applied, since maximum deformations result here due to the dominant self-weight (Figure 5a). The root-mean-square of the slope deviations (Figure 5b) results to $SD_{rms} = 0.97$ mrad that fulfils the limiting value of 1.25 mrad. Here, the overall value is used, since mirror elements are also accounted for. The concrete structure has comparatively low deformations. Hence, the mirror elements cause the dominant deformations and consequently slope deviations. Additionally, the tensile strength of the concrete structure is not exceeded for operation and survival state. This means, cracking of the structure is mathematically prohibited. For robustness demands, i.e. that no brittle failure occurs, additional reinforcements are needed.

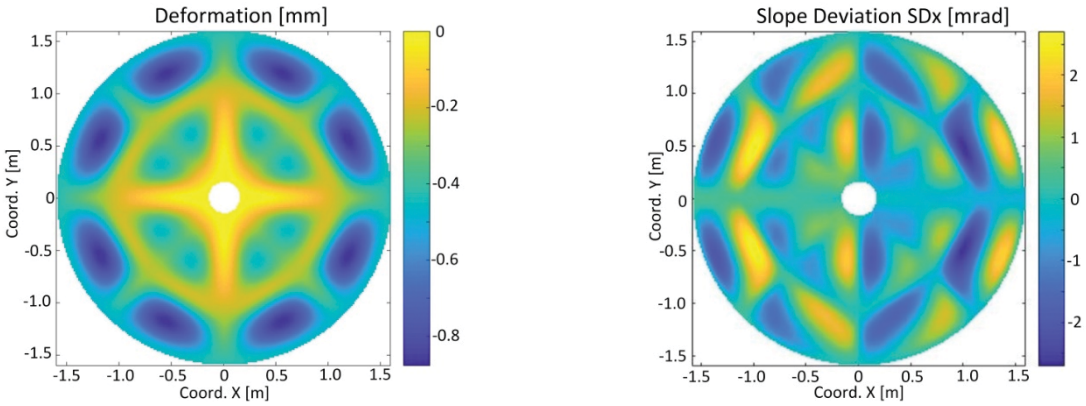

(a) (b)

FIGURE 5. (a) Numerically derived deformations, (b) Corresponding slope deviation in x-direction

CONSTRUCTION

The heliostat will be built up at the solar power tower plant Jülich (Germany). Therefore, the segmental modules are rigidly linked to an internal steel ring. This ring enables the tilting of the concentrator and is supported by an additional mounting structure (cf. Figure 6). Then, the mirror elements are applied. To evaluate the optical efficiency, the mirror surface will be photogrammetrically measured [13] and qualified.

Substructure

An already existing pylon is used for bearing. This pylon has been used before for a T-type steel heliostat collector at the solar power plant. Therefore, it consists of the actual pylon and a torque beam (traverse) that enabled the rotation and twisting of the initial steel concentrator (Figure 6, left). The connection between pylon and torque beam provided the rotation about the vertical axis. The torque beam is applied for tilting. To adopt this type of tracking for the aimed central mount support of the concrete concentrator, the bearing structure has to be elaborated. Therefore, two C-shaped steel structures have been designed that support the inner ring of the concrete concentrator and ensure the rotation. They are rigidly connected to the torque beam. The specific shape of this additional mounting enables the tracking without a collision between the radial beams and the substructure (Figure 6, right).

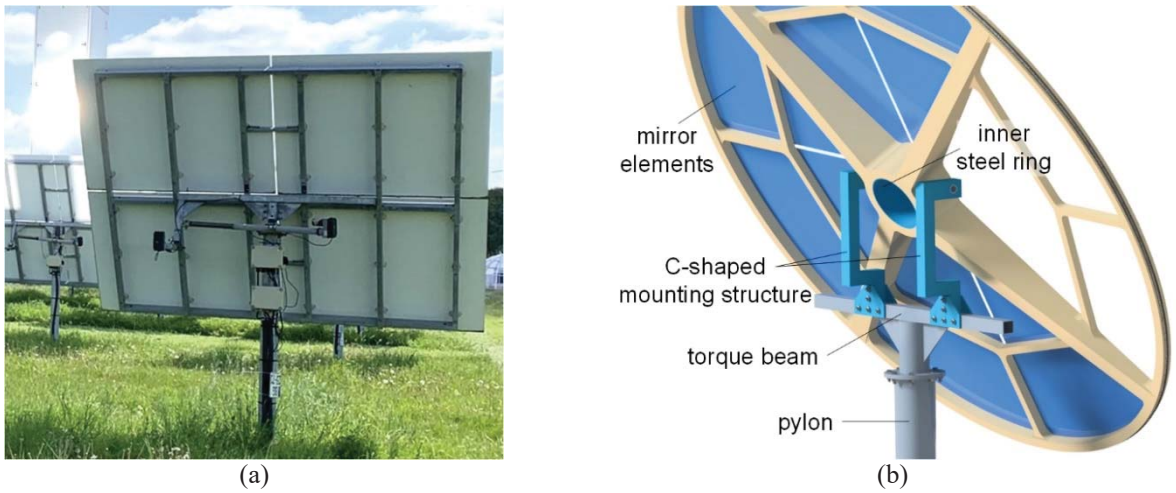

(a) (b)

FIGURE 6. a) Steel heliostat at the solar tower Jülich, b) Additional C-shaped mounting of the concrete collector

Concrete Concentrator

For concreting of the prototype, a formwork made from 3d-cut polystyrene is used to realize a precise geometry. The formwork consists of several modules to produce at least 4 modules. For a serial production, a stiffer and multiply reusable but more costly steel formwork is preferred. Figure 7a shows the formwork with installed reinforcement for robustness. Thereby, regular reinforcement bars with diameters of 8 mm are used but also micro-reinforcement meshes. The regular reinforcement ensures loading capacity and a ductile behavior in case of structural failure. The micro-reinforcements with diameters of 1 mm and a spacing of 1.5 cm bridge unintended cracks in local areas, e. g. due to stress peaks, so that low deformations are still observed for the whole structure. After concreting and hardening, the modules are stripped off and rigidly connected to the inner steel ring (Figure 7b). To attach the mirror elements, which are pre-sliced into the shape of almost isosceles triangles, threads are already embedded in the concrete modules. The mirror elements possess an angle of 45° meaning that two mirror elements are applied onto one module. A total of 8 mirror elements results that will be connected to the radial beams and secondary struts. Before the concrete heliostat will be erected and qualified at the solar tower Jülich, the functionality of the concrete collector is checked in a test set-up (Figure 8).

(a) (b)

FIGURE 7. (a) Modular polystyrene formwork with reinforcement detail, (b) concrete modules connected to the inner steel ring

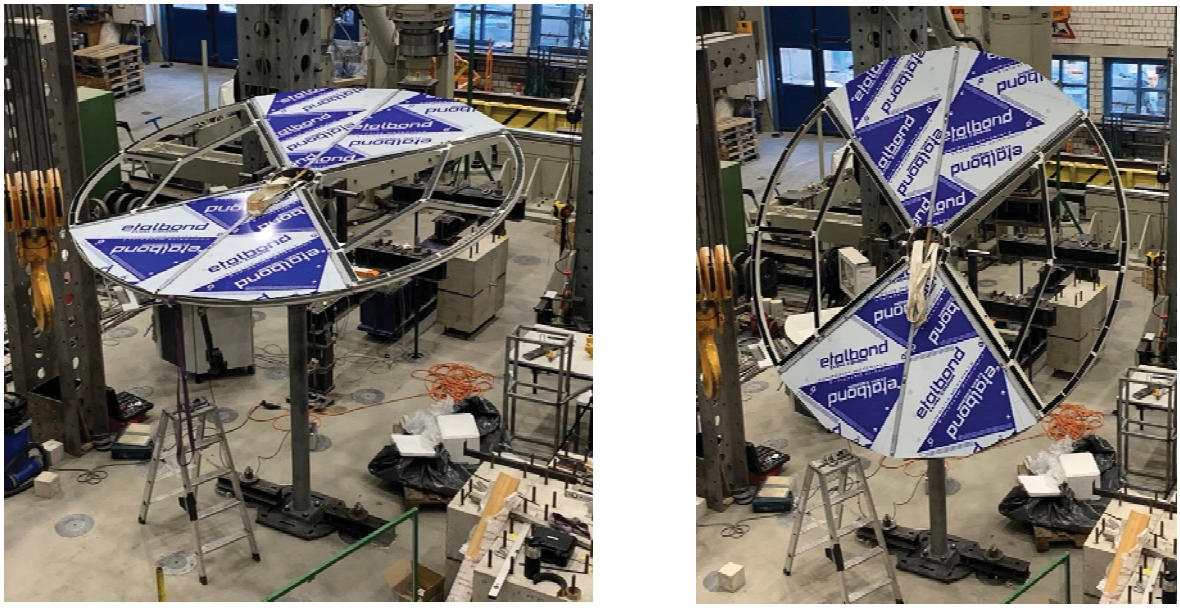

FIGURE 8. Test set-up of the concrete heliostat in the laboratory of TU Kaiserslautern, Germany

CONCLUSIONS AND OUTLOOK

The development of a concrete heliostat is presented. The main findings are:

- A modular structure subdivided into 90° 'pieces of cake' for a small-scale heliostat with an aperture area of 8 m² is derived. It possesses a total weight of 341 kg. This yields to an equivalent thickness of 1.8 cm only, i.e. the average thickness with respect to the aperture area.
- Concrete heliostats can be idealized as plates. By means of system reduction methods, rotationally symmetric modules are derived with respect to accuracy and material restrictions.
- Numerical analyses show that the main deformations arise for the mirror elements. However, they can easily be reduced by means of higher thicknesses of the mirrors but would come along with higher costs.
- The material costs for the reinforced concrete structure exhibits 11 €/m². Production costs are not considered yet. However, the heliostats are suitable for serial production so that required accuracy demands can be provided by inherent quality control and costs would reduce with the number of modules.
- The feasibility of the concrete collector has been proven in numerical analyses. The prototype will be erected at the solar tower Jülich (Germany) and qualified by means of photogrammetric measurement.
- A transfer to larger and more cost-effective collectors of approx. 30-40 m² seems possible. Hereby, circumferential post-tensioning to utilize the concrete's compressive strength should be applied [14].

ACKNOWLEDGMENTS

The authors thank the German Research Foundation (DFG) for its financial support of the 'knowledge transfer' project with the grant number 389020360. Sincere thanks are given to the project partners, especially Dr.-Ing. R. Buck, Dr.-Ing, K. Wieghardt, Dr.-Ing. habil. B. Sagmeister, Dipl.-Ing. T. Friedrich and Dr. R. Dasbach.

REFERENCES

1. https://www.solarpaces.org/csp-technologies/csp-projects-around-the-world, accessed: 20th September 2020
2. A. Pfahl, et al., Progress in heliostat development, Solar Energy **152**, 3-37 (2017).
3. M. Balz, V. Göcke, T. Keck, F. von Reeken, G. Weinrebe and M. Wöhrbach, "Stellio – Development, construction and testing of a smart heliostat", SolarPACES 2015 Conference, Cape Town, South Africa.
4. P. Forman, S. Penkert, C. Kämper, T. Stallmann, P. Mark and J. Schnell., "A survey of concrete shell collectors for parabolic troughs". Renewable and Sustainable Energy Reviews **134** (2020)
5. P. Forman, S. Penkert, D. Krüger, P. Mark, J. Schnell, K. Hennecke, J. Krüger and R. Dasbach, "A concrete solar collector – From design to assembly in full scale", VGB Powertech **9**, 42-48 (2018).
6. A. Belaid, A. Filali, A. Gama, B. Bezza, T. Arrif and M. Bouakba, "Design optimization of a solar tower power plant heliostat field by considering different heliostat shapes", International Journal of Energy Research, 1-18 (2020).
7. B. Sagmeister and G. Pahl, "Protective Layers made of UHPC", Bauingenieur **94(5)**, 179-183 (2019).
8. U. Winkelmann, C. Kämper, R. Höffer, P. Forman, M.A. Ahrens and P. Mark, "Wind actions on large-aperture parabolic trough solar collectors: Wind tunnel tests and structural analysis", Renewable Energy **146**, 230-2407 (2020).
9. B. Gong, Z. Wang, Z. Li, C. Zang and Z. Wu, "Fluctuating wind pressure characteristics of heliostats", Renewable Energy **50**, 307-316 (2013).
10. J.A. Peterka and R. Deickson, "Wind load design methods for ground-based heliostats and parabolic dish collectors", Technical Report SAND92-7009, Alberqueque, New Mexico, USA, 1992.
11. G. Markus and J. Otto, "Theorie und Berechnung rotationssymmetrischer Bauwerke", Werner, Düsseldorf, 1978.
12. L. Bocklenberg and P. Mark, "Thick slab punching with symmetry reductions", Structural Concrete **21**, 1-15 (2020).
13. K. Pottler, E. Lüpfert, G. H. G. Johnston and M. R. Shortis, "Photogrammetry: A powerful tool for geometric analysis of solar concentrators and their components", QSME 2004 International Solar Energy Conference, 719-726 (2004).
14. Forman, P.; Penkert, S.; Mark, P.; Schnell, J., "Design of modular concrete heliostats using symmetry reduction methods", Civil Engineering Design **2(4)**, 92–103 (2020).